Chinese Journal of Natural Medicines

Function-oriented synthesis of marine phidianidine derivatives as potent anti-MRSA agents

Qiong Wu, Bingyuan Yan, Chen Qu, Chao Ma, Xuwen Li

Citation: Qiong Wu, Bingyuan Yan, Chen Qu, Chao Ma, Xuwen Li, Function-oriented synthesis of marine phidianidine derivatives as potent anti-MRSA agents, Chinese Journal of Natural Medicines, 2026, 24(9), 1146-1152. doi: 10.1016/S1875-5364(26)61208-3.

View online: https://doi.org/10.1016/S1875-5364(26)61208-3

Related articles that may interest you

Diversity-oriented synthesis of marine sponge derived hyrtioreticulins and their anti-inflammatory activities

Chinese Journal of Natural Medicines. 2022, 20(1), 74-80 https://doi.org/10.1016/S1875-5364(22)60155-9

A comprehensive review of natural products with anti-hypoxic activity

Chinese Journal of Natural Medicines. 2023, 21(7), 499-515 https://doi.org/10.1016/S1875-5364(23)60410-8

A review of structural modification and biological activities of oleanolic acid

Chinese Journal of Natural Medicines. 2024, 22(1), 15-30 https://doi.org/10.1016/S1875-5364(24)60559-5

Anti-hepatitis B virus activities of natural products and their antiviral mechanisms

Chinese Journal of Natural Medicines. 2023, 21(11), 803-811 https://doi.org/10.1016/S1875-5364(23)60505-9

Synthesis and anti-HIV activities of phorbol derivatives

Chinese Journal of Natural Medicines. 2024, 22(2), 146-160 https://doi.org/10.1016/S1875-5364(24)60587-X

Synthesis, and anti-inflammatory activities of gentiopicroside derivatives

Chinese Journal of Natural Medicines. 2022, 20(4), 309-320 https://doi.org/10.1016/S1875-5364(22)60187-0

Wechat

Chinese Journal of Natural Medicines 24 (2026) 1146-1152

Contents lists available at ScienceDirect

Chinese Journal of Natural Medicines

journal homepage: www.cjnmcpu.com/

Original article

Function-oriented synthesis of marine phidianidine derivatives as potent anti-MRSA agents

Qiong Wu[a,b,Δ], Bingyuan Yan[a,d,Δ], Chen Qu[a], Chao Ma[b,*], Xuwen Li[a,c,d,*]

[a] *Shandong Laboratory of Yantai Drug Discovery, Bohai Rim Advanced Research Institute for Drug Discovery, Yantai 264117, China*
[b] *Key Laboratory of Structure-Based Drug Design & Discovery of Ministry of Education, School of Pharmaceutical Engineering, Shenyang Pharmaceutical University, Shenyang 110016, China*
[c] *State Key Laboratory of Chemical Biology, Shanghai Institute of Materia Medica, Chinese Academy of Sciences, Shanghai 201203, China*
[d] *School of Pharmacy, Shandong Second Medical University, Weifang 261053, China*

ARTICLE INFO

Article history:
Received 20 November 2025
Revised 23 February 2026
Accepted 27 February 2026
Available online 20 September 2026

Keywords:
Marine natural products
Phidianidines
Antibacterial activity
Structure-activity relationship

ABSTRACT

The rapid emergence of multidrug-resistant bacterial pathogens, particularly methicillin-resistant *Staphylococcus aureus* (MRSA), underscores the critical discovery for new antibiotics with novel scaffolds. We identified lead compound LXW933, which exhibits promising anti-MRSA activity and features a unique 1,2,4-oxadiazole scaffold, from our phidianidine-based compound library. Based on this structure, a Function-Oriented Synthesis (FOS) strategy had been conducted to afford a series of phidianidine derivatives for their antibacterial activity evaluation. Compounds **24a** exhibited excellent anti-MRSA efficacy with an MIC value of 1.5 μg/mL and low toxicity against HeLa cells. Further mechanistic study showed that **24a** effectively inhibits biofilm formation and exerts its antibacterial effect by disrupting the bacterial cell membrane. This research provides valuable insights for the discovery of antibacterial drug leads derived from oxadiazole-containing marine alkaloids, paving the way for new strategies to combat antimicrobial resistance.

1. Introduction

The relentless evolution of drug-resistant bacteria continues to undermine modern medicine's capacity to combat infectious diseases, posing one of the most critical challenges to global public health in the 21st century [1]. Among these pathogens, methicillin-resistant *Staphylococcus aureus* (MRSA) stands out due to its high virulence and multidrug-resistant phenotype [2]. This super-resistant bacterium not only causes severe and often life-threatening infections but also demonstrates an expanding resistance profile, rendering conventional antibiotics increasingly ineffective [3,4]. Compounding this threat is the slow pace of novel antibiotic development, which lags far behind the rapid adaptation of bacterial resistance, thereby deepening the global health crisis [5]. The World Health Organization has warned that, without effective intervention, antimicrobial resistance could cause over 10 million deaths annually by 2050 [6]. In light of this urgent challenge, the discovery of antimicrobial agents with novel chemical scaffolds and distinct mechanisms of action has become a paramount objective in pharmaceutical research [7,8].

Marine natural products, characterized by their structural diversity and broad biological activities, represent a promising source for new drug leads [9,10]. Our group has long been dedicated to the exploration of bioactive marine natural products [11-15]. Phidianidines A and B (Fig. 1), a unique class of indole alkaloids isolated from the marine opisthobranch mollusk *Phidiana militaris*, were the first reported marine natural products incorporating a 1,2,4-oxadiazole ring system [16]. Subsequent pharmacological evaluations have revealed that phidianidines and their synthetic analogs exhibit a wide range of bioactivities, including multifunctional neuroprotection [17], PTP1B inhibition [18], antifouling activities [19], selective dopamine transporter inhibitory, μ-opioid receptor antagonism [20], anti-oxidative [21], anti-inflammatory activity [22] and immunosuppressive [23]. In fact, a wealth of bioactive natural products and synthetic drugs incorporate the oxadiazole ring as a key pharmacophore, and numerous 1,2,4-oxadiazole-containing compounds have demonstrated promising antibacterial activities. For example, O'Daniel and co-workers discovered a novel class of non-β-lactam antibiotics, 1,2,4-oxadiazole derivatives **1**, which exhibited exceptional anti-MRSA activity [24]. More recently, Barbachyn and co-workers developed a novel 1,2,4-oxadiazole derivative **2** exhibiting high selectivity and potent activity against *Clostridioides difficile* — a Gram-positive bacterium and a leading cause of antibiotic-associated diarrhea worldwide (Fig. 1) [25]. Inspired by these findings and the demonstrated antibacterial potential of the 1,2,4-oxadiazole scaffold, we screened our pre-established compound library of marine-derived phidianidine derivatives for antibacterial activity leading to the identification of lead compound LXW933 [22,23], which displayed promising antibacterial activity (MIC 6 μg·mL^{-1} against MRSA (ATCC 43300), Fig. 1). The structure of compound LXW933 was designed by replacing the guanidine side-chain of phidianidine B with a 2,2,2-spiro ring and a phenoxybenzenesulfonamide (POBSA) fragment. To further improve its potency, we conducted four rounds of rational

* Corresponding author.
E-mail addresses: machao_syphu@163.com (C. Ma); xwli@simm.ac.cn (X. Li)
Δ These authors contributed equally to this work.

https://doi.org/10.1016/S1875-5364(26)61208-3
Copyright © 2026, China Pharmaceutical University. Published by Elsevier B.V. All rights reserved.

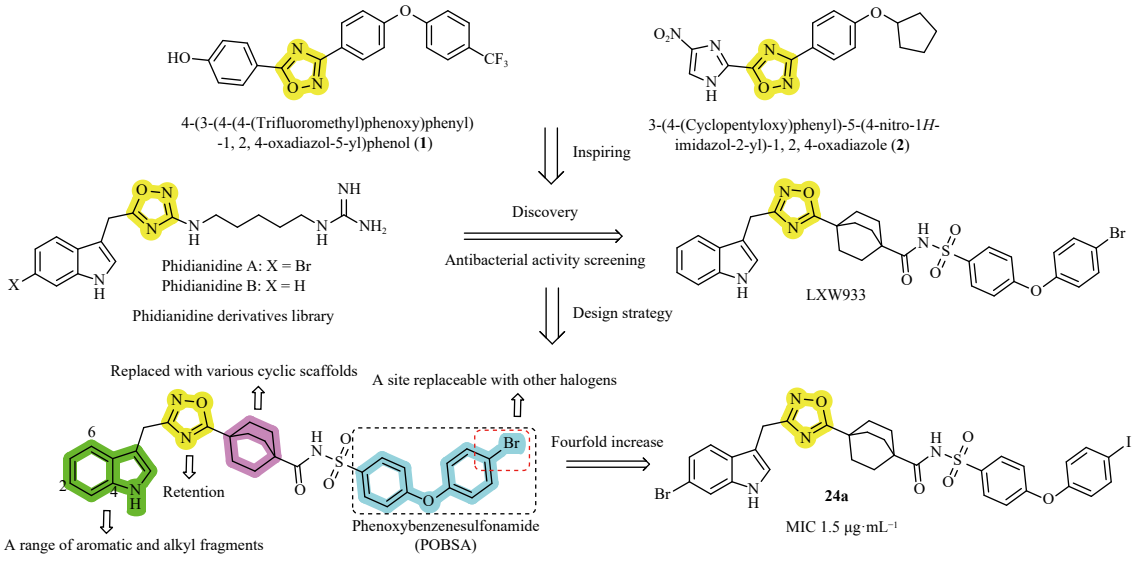


Fig. 1 Structures of compounds **1**, **2**, LXW933 and phidianidines, and design strategy for new phidianidine derivatives.

structural modification, synthesizing novel derivatives and evaluating their MIC values and conducted an analysis of their structure-activity relationships (SAR).

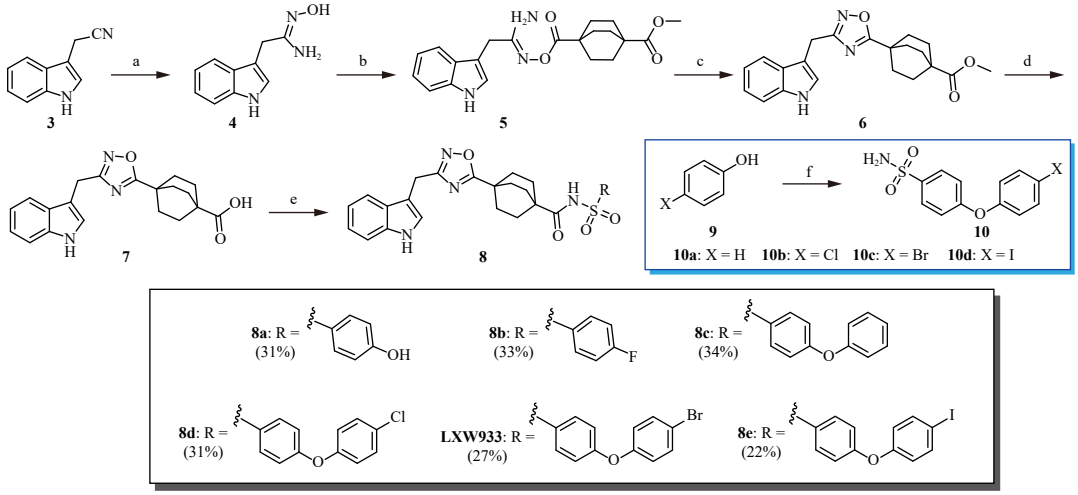
2. Results and discussion

2.1. Chemistry

The structural optimization work was initiated based on the structure of lead compound LXW933. Our initial structural modification focused on the Br-substituted phenoxybenzenesulfonamide (POBSA) fragment (highlighted in light blue, Fig. 1), a site replaceable with other halogens. In the second round, the 2,2,2-spiro ring (highlighted in purple, Fig. 1) was replaced with various cyclic scaffolds. The third round further diversified the scaffold by replacing the indole ring (highlighted in green, Fig. 1) with a range of aromatic and alkyl fragments. The final round combined the most favorable structural fragment identified in the previous stages to produce compounds with improved antimicrobial activity.

In the first round, we substituted the Br atom of POBSA fragment with other halogens or replaced the entire POBSA fragment with diverse substituted benzene rings. As shown in Scheme 1, the route proceeds by reacting 3-indoleacetonitrile **3** with $NH_2OH{\cdot}HCl$ and $NaHCO_3$ in EtOH to afford amidoxime **4**. Esterification of **4** with carboxylic acid ester by using 2-(7-azabenzotriazol-1-yl)-*N*,*N*,*N*′,*N*′-tetramethyluronium hexafluorophosp hate (HATU) and diisopropylethylamine (DIPEA) in CH_2Cl_2 gave intermediate **5**. Then, an intramolecular cyclization of **5** in the presence of sodium acetate (NaOAc) in 30 % EtOH (in H_2O) under reflux led to the oxadiazole compound **6**. Compound **6** was then hydrolyzed using a 1∶1 mixture of saturated NaOH solution and ethanol, affording carboxylic acid **7**. On the other hand, phenol derivative **9** underwent an SNAr reaction with 4-fluorobenzenesulfonamide and Cs_2CO_3 in DMSO to yield POBSA derivative **10**. Finally, either compound **10**, 4-hydroxybenzenesulfonamide, or 4-fluorobenzenesulfonamide was subjected to an amide condensation with carboxylic acid **7** under HATU and DIPEA mediation, yielding compound **8**.

Based on the bioactivity data from the initial round of modifications, the halogen-substituted POBSA moiety was confirmed as the critical pharmacophore for this series, with the iodo-substituted analogue demonstrating the highest potency (**8e**). However, due to unsatisfactory synthetic yields (15% for **10d** *vs* 30% for **10c**), the Br-substituted POBSA analogue, which main-



Scheme 1 Reagent and conditions: (a) $NH_2OH{\cdot}HCl$, $NaHCO_3$, EtOH, reflux, 5 h. (b) carboxylic acid ester, HATU, DIPEA, CH_2Cl_2, rt, 3 h. (c) NaOAc, 30 % EtOH, reflux, overnight. (d) NaOH (aq.)/EtOH (1∶1, *V*/*V*), rt, overnight. (e) for **8d**, LXW933, and **8e**: **10**, HATU, DIPEA, CH_2Cl_2, rt, overnight; for **8a**–**8c**: benzene sulfonamide derivatives, HATU, DIPEA, CH_2Cl_2, rt, overnight; (f) 4-fluorobenzene-sulfonamide, Cs_2CO_3, DMSO, 135 °C, 12 h.

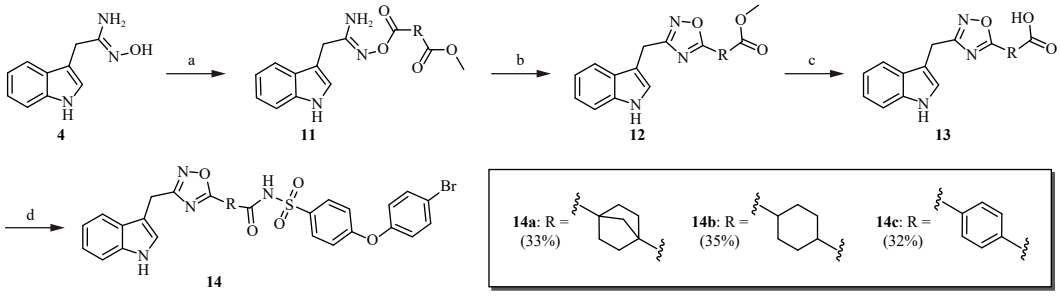
tained comparable potency, was selected as the privileged fragment for subsequent development. In the second round of modification, we focused on optimizing the central spiro ring system. By replacing the original spiro ring with various cyclic scaffolds, we designed and synthesized a series of novel derivatives **14**, as displayed in Scheme 2. The synthetic approach for these compounds largely follows the route outlined in Scheme 1. Amidoxime **4** was first esterified with a series of carboxylic acids to provide intermediate **11**. Then, an intramolecular cyclization of **11** led to the oxadiazole compound **12**, which was hydrolysed to produce **13**. Finally, condensation of **13** with compound **10c** using standard amide coupling conditions yielded the target compound **14**.

Building on the second-round results, which identified the 2,2,2-spiro ring as a key pharmacophore, we performed a third round of structural modifications. In the third round, the indole ring was substituted with a range of other aromatic fragments, modified indole rings, and alkyl fragments to assess the effect on antibacterial potency. Diverging from the strategy in Scheme 1, which initiates from the indole moiety, the present route commences with the Br-substituted POBSA fragment, enabling efficient assembly of the target analogues, as illustrated in Scheme 3. First, compound **10c** was subjected to amidation with a carboxylic acid ester, affording intermediate **15**, which subsequently was hydrolysed to give **16**. Meanwhile, diverse acetonitrile-derived derivatives **18** were converted to the corresponding amidoximes **19**, which was then esterified with carboxylic acid **16** to yield **17**. Finally, cyclization under reflux with sodium acetate yielded the 1,2,4-oxadiazole ring, furnishing the target product **20**.

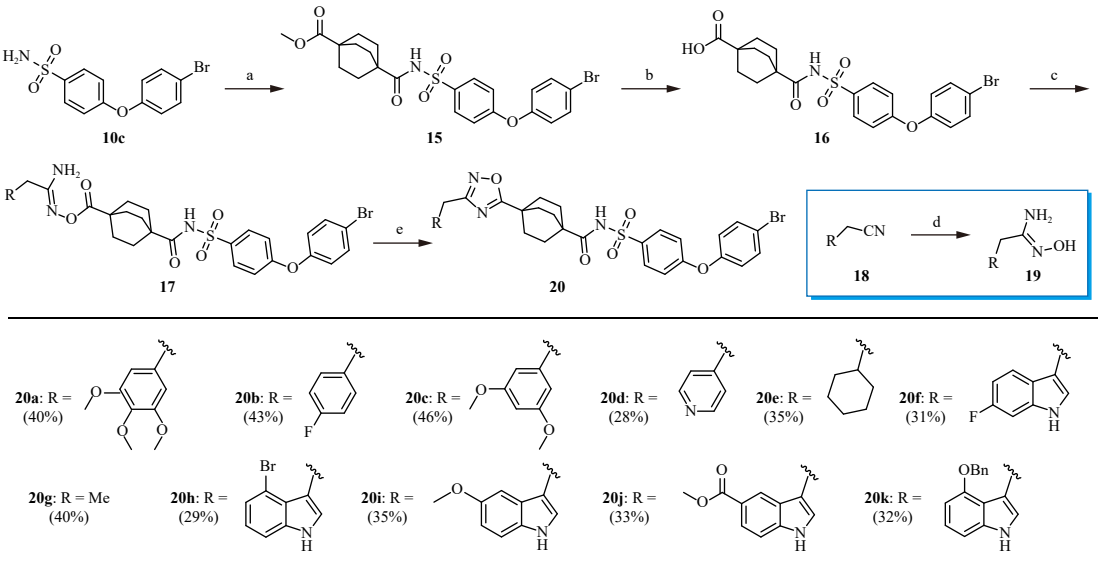
Activity results revealed that replacement of the indole ring with other ring systems led to diminished activity, whereas the introduction of F at the C_2-position of indole enhanced activity (**20f**). Consequently, we postulated that other halogens at this position might yield even greater potency. Furthermore, our first round of modifications had already established that the iodo-substituted POBSA fragment was optimal. Based on this, we designed and synthesized three compounds by incorporating indole rings substituted at the C_2-position with different halogens (F, Cl, Br) and the iodo-substituted POBSA fragment. Its synthesis followed the route outlined in Scheme 3, as showed in Scheme 4.

2.2. Antibacterial activity

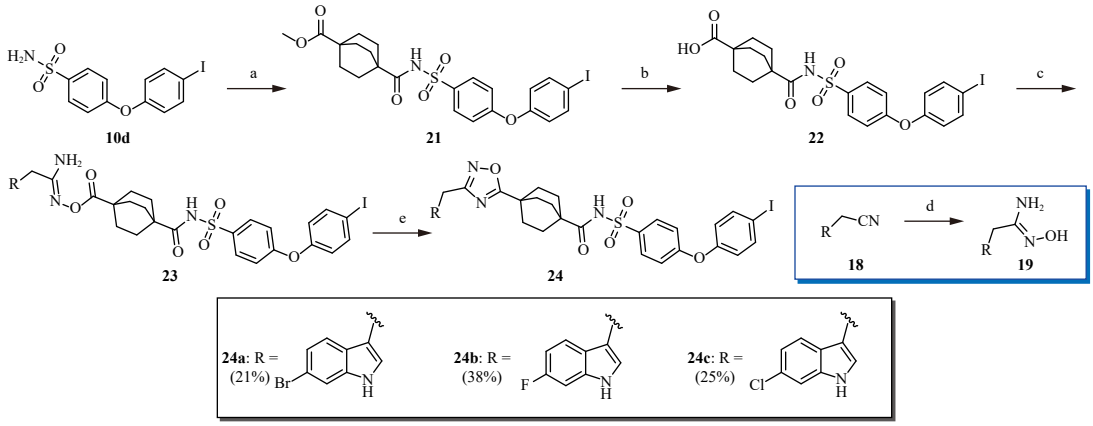
The *in vitro* antibacterial activities of the synthesized phidianidine derivatives **8a–8e**, **14a–14c**, **20a–20k**, **24a–24c**, and two related intermediates **16**, **22** were evaluated against a panel of clinically relevant bacterial strains using a standardized broth microdilution method in accordance with CLSI guidelines. Chloramphenicol was used as a positive control. The tested strains included three Gram-positive bacteria—*S. aureus* (ATCC 6538 and MRSA ATCC 43300), and *E. faecalis* (ATCC 29212), as well as two Gram-negative bacteria—*E. coli* (ATCC 25922) and *P. aeruginosa* (ATCC 27853). The results revealed that the synthesised phidianidine derivatives exhibits potent and selective activity against MRSA ATCC 43300 (Table 1). Notably, compound **24a** showed the highest potency with an MIC value of 1.5 μg·mL^{-1} against MRSA (ATCC 43300), along with clinically relevant activ-



Scheme 2 Reagent and conditions: (a) carboxylic acid ester derivatives, HATU, DIPEA, CH_2Cl_2, rt, 3 h. (b) NaOAc, 30 % EtOH in H_2O, reflux, overnight. (c) NaOH (aq.)/EtOH (1∶1, *V*/*V*), rt, overnight. (d) **10c**, HATU, DIPEA, CH_2Cl_2, rt, overnight.



Scheme 3 Reagent and conditions: (a) carboxylic acid ester, HATU, DIPEA, CH_2Cl_2, rt, overnight. (b) NaOH (aq.)/EtOH (1∶1, *V*/*V*), rt, overnight. (c) **19**, HATU, DIPEA, CH_2Cl_2, rt, 3 h. (d) acetonitrile derivatives, $NH_2OH{\cdot}HCl$, Na_2CO_3, EtOH, reflux, 5 h. (e) NaOAc, 30 % EtOH in H_2O, reflux, overnight.



Scheme 4 Reagent and conditions: (a) carboxylic acid ester, HATU, DIPEA, CH_2Cl_2, rt, overnight. (b) NaOH (aq.)/EtOH (1∶1, *V*/*V*), rt, overnight. (c) **19**, HATU, DIPEA, CH_2Cl_2, rt, 3 h. (d) acetonitrile derivatives, $NH_2OH{\cdot}HCl$, Na_2CO_3, EtOH, reflux, 5 h. (e) NaOAc, 30 % EtOH in H_2O, reflux, overnight.

Table 1 Antibacterial activity of phidianidine derivatives against MRSA (ATCC 43300), *S. aureus* (ATCC6538), *E. faecalis* (ATCC29212), *P. aeruginosa* (ATCC 27853), *E. coli* (ATCC25922).

Compound	MIC (μg·mL^{-1})				
	MRSA (ATCC43300)	*S. aureus*	*E. faecalis*	*P. aeruginosa*	*E. coli*
8a	> 64	> 64	> 64	> 64	> 64
8b	> 64	> 64	> 64	> 64	> 64
8c	> 64	16	32	> 64	> 64
8d	12	8	32	> 64	> 64
8e	4	32	16	> 64	> 64
14a	16	8	32	> 64	> 64
14b	16	16	32	> 64	> 64
14c	8	8	8	> 64	> 64
20a	> 64	16	64	> 64	> 64
20b	8	8	16	> 64	> 64
20c	8	8	32	> 64	> 64
20d	> 64	> 64	> 64	> 64	> 64
20e	8	8	16	> 64	> 64
20f	4	4	8	> 64	> 64
20g	> 64	> 64	> 64	> 64	> 64
20h	16	4	8	> 64	> 64
20i	8	8	16	> 64	> 64
20j	6	8	8	> 64	> 64
20k	6	8	8	> 64	> 64
24a	1.5	4	8	> 64	> 64
24b	2	4	8	> 64	> 64
24c	2	4	8	> 64	> 64
16	> 64	> 64	> 64	> 64	> 64
22	> 64	> 64	> 64	> 64	> 64
LXW933	6	4	16	> 64	> 64
Chloramphenicol	16	1	16	32	16

ity against *S. aureus* (MIC = 4 μg·mL^{-1}) and *E. faecalis* (MIC = 8 μg·mL^{-1}), while it was inactive against the tested Gram-negative bacteria (MIC > 64 μg·mL^{-1}). Furthermore, compounds **8e** (MIC = 4 μg·mL^{-1}), **20f** (MIC = 4 μg·mL^{-1}), **24b** (MIC = 2 μg·mL^{-1}), and **24c** (MIC = 2 μg·mL^{-1}) also exhibited potent activity against MRSA (ATCC 43300). Additionally, **24a**, **24b** and **24c** were further evaluated against additional clinically relevant strains, including MRSA (ATCC 33591), MRSA (USA300), and MSSA (ATCC 4420). Both compounds **24a** and **24b** exhibited potent activity against these three strains, with MIC values of 2 μg·mL^{-1} (Table 2).

Table 2 Antibacterial activity of **24a**, **24b**, and **24c** against MRSA (ATCC33591), MRSA (USA300), MSSA (ATCC4420).

Compound	MIC (μg·mL^{-1})		
	MRSA (ATCC33591)	MRSA (USA300)	MSSA (ATCC4420)
24a	2	2	2
24b	2	2	2
24c	8	2	4
LXW933	12	12	12

2.3. Structure-activity relationships (SAR)

Through systematic analysis of the antimicrobial activity results, we have established the following SAR (Fig. 2). Firstly, the halogen-substituted POBSA moiety was confirmed as the critical pharmacophore for this series, as compounds lacking this modification (**8a–8c**) were completely inactive against MRSA ATCC43300 (MIC > 64 μg·mL^{-1}). More intriguingly, the identity of the halogen atom at this position demonstrated a clear correlation with antibacterial potency, following the trend: Cl (**8d**, MIC = 12 μg·mL^{-1}) < Br (lead compound LXW933, MIC = 6 μg·mL^{-1}) < I (**8e**, MIC = 4 μg·mL^{-1}). Furthermore, the 2,2,2-spiro ring proved to be a privileged pharmacophore; replacement of the 2,2,2-spiro ring with other ring systems—such as the 2,2,1-spiro ring (**14a**), cyclopropyl (**14b**), or a benzene ring (**14c**)—led to a slight reduction in activity. Finally, the indole ring was established as the privileged pharmacophore for this series. Substitutions on the indole ring with groups such as trimethoxyphenyl (**20a**), pyridine (**20d**), or methyl (**20g**) led to a complete loss of antibacterial activity. Additionally, substitutions with 4-fluorophenyl (**20b**), 3,5-dimethoxyphenyl (**20c**) or cyclohexyl (**20e**) reduced the activity to an MIC of 8 μg·mL^{-1}. Studies indicated that only halogen at the C_2 position of the indole ring enhanced antibacterial activity, with the 2-fluoro derivative (**20f**) achieving an MIC of 4 μg·mL^{-1}. Notably, the combination of the iodo-substituted POBSA and the 2-Br-substituted indole afforded the preferred compound **24a**, which exhibited a significantly enhanced synergistic

effect, reducing the MIC against MRSA (ATCC43300) to 1.5 μg·mL^{-1}.

2.4. Antibiofilm assay

To gain deeper insight into its antibacterial mechanism, we first evaluated the ability of compound **24a** to inhibit MRSA (ATCC43300) biofilm formation, using the crystal violet (CV) staining method. As shown in Fig. 3B, at a concentration of 1.5 μg·mL^{-1}, **24a** achieved over 80 % inhibition of biofilm formation, indicating that this compound can effectively disrupt biofilm formation even at a low concentration. We next probed its effect on bacterial membrane integrity by dual-fluorescence staining with *N*,*N*-dimethylaniline *N*-oxide (DMAO) and propidium iodide (PI). DMAO labels all bacteria (regardless of viability), whereas PI only enters those with damaged membranes. As depicted in Fig. 3A, untreated MRSA (ATCC43300) exhibited exclusively green DMAO fluorescence, confirming membrane integrity and cell viability. In contrast, treatment with **24a** resulted in intense red PI fluorescence, demonstrating that **24a** disrupts the MRSA (ATCC43300) cell membrane, leading to bacterial death. Notably, further investigation revealed that this membrane disruption occurs without significant dissipation of the membrane potential (Fig. S89), suggesting a mechanism distinct from generalized depolarization.

2.5. Bactericidal time-kill kinetics

To further characterize its bactericidal efficacy, we evaluated compound **24a** at three concentrations in time-kill kinetics assays against MRSA (ATCC43300) over 12 h. As shown in Fig. 3C, while the bacterial count in the control group increased exponentially, treatment with **24a** at 2× MIC reduced it below the detection limit within 5 hours. Further increasing the concentration to 4× MIC achieved this effect within 3 h. Overall, compound **24a** displayed rapid, concentration-dependent bactericidal activity against MRSA (ATCC43300) and demonstrated superior rapid killing performance compared to chloramphenicol at 4× MIC.

2.6. Cytotoxicity

To assess the preliminary safety profile of the active derivatives, the cytotoxicity of compounds **24a**, **24b**, and **24c** was evaluated against human cervical carcinoma (HeLa) cells using the Cell Counting Kit-8 (CCK-8) assay. Following 24 h of HeLa cell culture, cell suspensions were treated with varying concentrations of the test compounds and reference drugs. Viability was assessed by measuring the optical density at 450 nm (OD_{450}). As demonstrated in Fig. 3D, the compounds exhibited no significant cytotoxicity toward HeLa cells, with cell viability remaining comparable to the blank control group, indicating favorable biocompatibility.

2.7. Compound characterization

24a was obtained as a light yellow syrup. The HR-ESI-MS spectrum displayed a pseudo molecular ion peak at *m/z* 787.0064 $[M + H]^+$, consistent with the molecular formula $C_{32}H_{29}BrIN_4O_5S$. The ^{1}H NMR spectrum of compound **24a** exhibited a characteristic singlet at δ_H 4.14 (2H), which was assigned to the methylene bridge (-CH_2-) connecting the indole and oxadiazole rings; The presence of the spiro scaffold was unambiguously confirmed by two distinct sets of aliphatic multiplets at δ_H 2.04–1.94 (m, 6H) and 1.83–1.77 (m, 6H), which are diagnostic for the protons on the spiro-aliphatic rings; The aromatic region displayed two characteristic coupling systems at δ_H 7.99 (d, 2H)/7.03 (d, 2H) and 7.71 (d, 2H)/6.84 (d, 2H), which are consistent with the presence of the POBSA moiety. The ^{13}C NMR spectrum displayed 32 carbon resonances, including a carbonyl carbon at δ_C 183.9, oxadiazole C=N carbons at δ_C 169.2 and 162.1, and a quaternary carbon bearing iodine at δ_C 88.7. In the HSQC spectrum, all protonated carbons were unambiguously correlated with their respective protons, including the methylene and aliphatic ring protons (Fig. S81). Collectively, these spectroscopic data provide comprehensive evidence for the proposed structure of **24a**.

3. Conclusions

In summary, we performed four rounds of structural modifications, based on the lead compound LXW933, which was identified from our in-house phidianidine-based compound library, and designed and synthesized 24 novel derivatives. The most promising compound **24a**, demonstrated significant anti-MRSA activity with an MIC of 1.5 μg·mL^{-1}, and low toxicity. The SAR study revealed that the iodo-substituted POBSA fragment, 2-Br indole fragment and the 2,2,2-spiro ring were beneficial to increase the antibacterial activity. Moreover, further mechanism of action studies revealed that compound **24a** effectively inhibits biofilm formation and exerts its antibacterial effect by disrupting the bacterial cell membrane. Compound **24a** could represent a promising lead compound for combating MRSA, also offering valuable

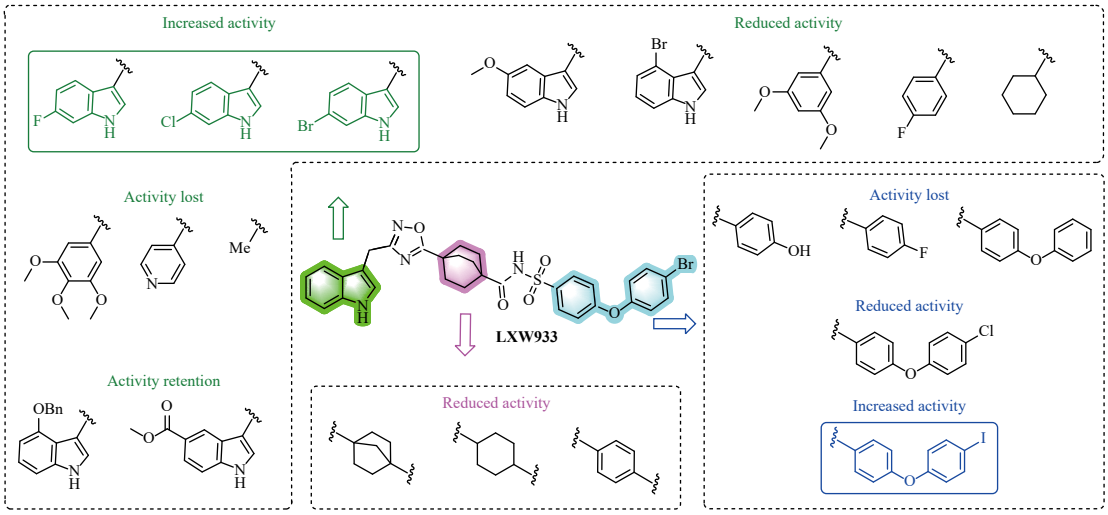


Fig. 2 SAR analysis of phidianidine derivatives.

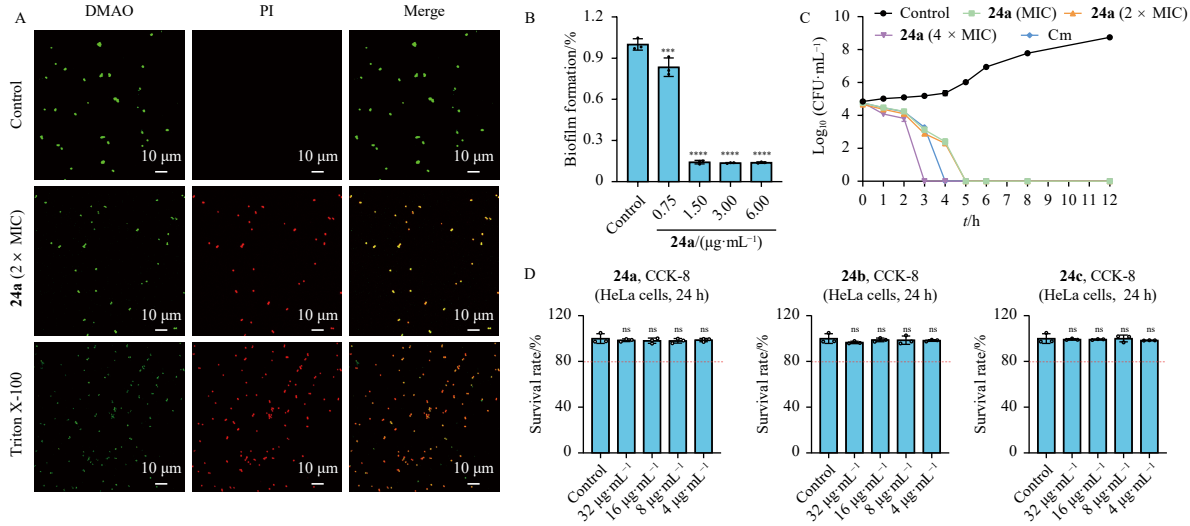


Fig. 3 (A) Fluorescence micrographs of MRSA (ATCC43300) cells stained with DMAO and PI and treated with **24a** (3 μg·mL^{-1}) and TritonX-100 (1 %). Control: no treatment. (B) Eradication of MRSA (ATCC43300) preformed biofilm was determined by the crystal violet staining method. (C) Time-kill curves of MRSA (ATCC43300) with compound **24a** and Chloramphenicol. (D) Cytotoxicity of **24a**, **24b** and **24c** against HeLa cells at 24 h. The bar data are in means ± SEM of three individual experiments in which each was performed in triplicate. A significant difference between the control group and the treatment group was indicated by asterisks : $^{***}P < 0.001$ and $^{****}P < 0.0001$.

insights for the development of marine-derived oxadiazole-based scaffolds against drug-resistant bacterial infections.

4. Experimental

4.1. General information

All reagents and solvents were purchased from common commercial suppliers and were used without further purification. ^{1}H NMR spectra were recorded at 600 MHz and ^{13}C NMR were recorded at 150 MHz on a Bruker NMR spectrometer instrument (AVANCE NEO). All ^{1}H NMR shifts are reported in δ units relative to the signals for $CDCl_3$ (7.26), CD_3OD (3.31) and DMSO-d_6 (2.50). HR-ESI-MS spectra were recorded on Waters VION IMSQTOF. Precoated silica gel GF254 plates (Sinopharm Chemical Reagent Co., Shanghai, China) were used for analytical TLC. Reversed-phase (RP) HPLC was performed on an Agilent 1260 series liquid chromatography equipped with a 1260 DAD WRG7115A detector at 210 and 254 nm. An Agilent semipreparative XDB-C18 column (5 μm, 9.4 mm × 250 mm) was employed for the purification. All solvents used for column chromatography and HPLC were of analytical grade (Shanghai Chemical Reagents Co., Ltd.) and chromatographic grade (Dikma Technologies Inc.), respectively.

4.2. Minimum inhibitory concentration (MIC)

The MIC was determined by broth microdilution according to Clinical and Laboratory Standards Institute (CLSI) guidelines [26]. The test medium was cation-adjusted Mueller-Hinton broth (CAMHB). Two-fold serially diluted drug concentrations were tested using a 96-well plate, which was inoculated with a bacterial cell concentration of approximately 1 × 10^5 colony formation unit (CFU). After 20 h of incubation at 37 °C statically, microbial growth in the dilution series was analysed. The MIC was defined as the minimum concentration of antibiotic at which no visible bacterial growth was observed. The experiment was conducted in triplicate.

4.3. Cytotoxicity assay

Cytotoxicity assays were conducted using the human cervical cancer cell line (HeLa). HeLa cells were cultured in (Dulbecco's Modified Eagle Medium) DMEM medium supplemented with 10% foetal bovine serum (FBS) and 1% penicillin/streptomycin at 37 °C in a 5% CO_2 incubator. The HeLa cell line was seeded at a density of 1 × 10^4 cells per well in a 96-well plate and incubated at 37 °C under 5% CO_2 overnight. Cells were treated with compounds at varying concentrations and incubated for 24 h. Cell viability was measured using the Cell CCK-8 from (Taoshu Shanghai, China) according to the manufacturer's protocol.

4.4. Antibiofilm assay

Biofilm inhibition was assessed using the crystal violet staining method in 96-well microtiter plates [27]. Briefly, overnight cultures of MRSA (ATCC43300) were diluted in fresh MH medium to an OD600 of 0.01 and inoculated into sterile 96-well plates, with three replicate wells per concentration. Test compounds at various concentrations were added, using an equal volume of DMSO as the solvent control. After 24 h of incubation at 37 °C, the medium was aspirated, and the plates were gently washed twice with PBS to remove non-adherent cells. The adherent biofilm was stained with 0.5% crystal violet for 15 min at room temperature. After rinsing three times with PBS to remove excess dye, the bound dye was solubilized with 95% ethanol. The absorbance was measured at 595 nm using a SpectraMax i3x microplate reader (Molecular Devices). The biofilm formation in each group was normalized to that of the DMSO control (set as 100%). All experiments were performed in triplicate wells and independently repeated three times.

4.5. Live-Dead staining assay

The viability of MRSA (ATCC43300) within biofilms was assessed using a bacterial viability kit containing two fluorescent dyes, DMAO and PI. After treating the biofilms with varying concentrations of the test compound for 4 hours at 37 °C, non-adherent bacterial cells were removed by washing twice with PBS. The biofilms were then dual-stained with DMAO and PI for 30 minutes at room temperature in the dark. After washing to remove excess dye, the samples were visualized by confocal laser scanning microscopy (CLSM). Multiple random fields were examined for each sample. Bacteria with intact membranes fluoresced green (DMAO), whereas those with compromised membranes fluoresced red due to PI uptake.

4.6. Time-killing assays

A mid-logarithmic phase culture of MRSA (ATCC 43300) was adjusted to about 1 × 10^5 CFU·mL^{-1} and treated with compound **24a** at 1× , 2× , and 4× MIC, using Chloramphenicol (4× MIC) as a positive control. The cultures were incubated at 37 °C with shaking. At designated time points (0, 1, 2, 3, 4, 5, 6, 8, and 12 h), aliquots were withdrawn, serially diluted, and spot-plated on MH agar for viable colony enumeration after 16–24 h. Time-kill curves were generated by plotting $\log_{10}$ CFU·mL^{-1} against time.

4.7. Cytoplasmic Membrane Depolarization Assay

Membrane potential was measured by DiSC3(5) (3,3'-dipropylthiadicarbocyanineiodide) dye method [28]. The bacteria in the exponential growth phase was washed with sterile PBS once, and suspended in the buffer composed with 5 mmol·L^{-1} HEPES, 5 mmol·L^{-1} glucose, 5 mmol·L^{-1} KCl (1∶1∶1, pH 7.2), adjusting the OD_{600} to 0.6. 130 μL bacterial suspensions were distributed into 96-well black plate (Costar), followed with addition of 2.5 μL DiSC3(5) dye (150 μmol·L^{-1} stock solution, dissolved in DMSO).The mixtures were incubated for 3 min at room temperature. Then, the test compounds were added to the bacterial suspension at the final working concentration of 6–0.75 μg·mL^{-1}. Each test was performed in triplicate. The fluorescence was monitored at 25 °C at one minute interval using the microplate reader with an excitation wavelength of 595 nm and an emission wavelength of 665 nm.

Funding

This work was supported by the Key R&D Program of Shandong Province (Nos. 2024CXPT028 and 2025CXPT012), the National Key Research and Development Program of China (No. 2021YFF0502400), the Strategic Priority Research Program of the Chinese Academy of Sciences (No. XDB1060000), and Taishan Scholars Program (tsqn2023-12302), the Natural Science Foundation of China (Nos. 42576087), 2025 Annual Self-deployment Project of State Key Laboratory of Chemical Biology (No. SKLCB-2025-06), the Fundamental Research Projects of Science & Technology Innovation and Development Plan in Yantai City(No. 2023JCYJ057).

Supporting Information

Supporting information can be requested by sending E-mail to the corresponding authors.

Declaration of competing interest

These authors have no conflict of interest to declare.

References

1 Antimicrobial Resistance Collaborators. Global burden of bacterial antimicrobial resistance in 2019: a systematic analysis. *Lancet*. 2022;399 (10325):629-655. https://doi.org/10.1016/S0140-6736(21)02724-0.
2 Chen QQ, Ding YH, Li ZY, et al. Comprehensive analysis of the antibacterial activity of 5,8-dihydroxy-1,4-naphthoquinone derivatives against methicillin-resistant *Staphylococcus aureus*. *Chin J Nat Med*. 2025;23(5):604-613. https://doi.org/10.1016/S1875-5364(25)60818-1.
3 Smith WPJ, Wucher BR, Nadell CD, et al. Bacterial defences: mechanisms, evolution and antimicrobial resistance. *Nat Rev Microbiol*. 2023;21(8):519-534. https://doi.org/10.1038/s41579-023-00877-3.
4 Ampomah-Wireko M, Qu Y, Li D, et al. Design, synthesis and antibacterial evaluation of oxazolidinone derivatives containing *N*-methylglycyl or quaternary ammonium salts. *Bioorg Med Chem*. 2025;122:118144. https://doi.org/10.1016/j.bmc.2025.118144.
5 Kong QD, Yang YS. Recent advances in antibacterial agents. *Bioorg Med Chem Lett*. 2021;35:127799. https://doi.org/10.1016/j.bmcl.2021.127799.
6 Kokot M, Anderluh M, Hrast M, et al. The structural features of novel bacterial topoisomerase inhibitors that define their activity on topoisomerase IV. *J Med Chem*. 2022;65(9):6431-6440. https://doi.org/10.1021/acs.jmedchem.2c00039.
7 Wu J, Song T, Zhang L, et al. Antibacterial and cytotoxic metabolites produced by *Streptomyces tanashiensis* BYF-112 isolated from *Odontotermes formosanus*. *Chin J Nat Med*. 2024;22(9):822-830. https://doi.org/10.1016/s1875-5364(24)60720-x.
8 Zhao SF, Jing ZW. New pimarane diterpenoids with antibacterial activity from fungus Arthrinium sp. ZS03. *Chin J Nat Med*. 2024;22(4):356-364. https://doi.org/10.1016/S1875-5364(24)60629-1.
9 Huang C, Jing Y, Fu PP, et al. Discovery of novel small molecules targeting hepatitis B virus core protein from marine natural products with HiBiT-based high-throughput screening. *Acta Pharm Sin B*. 2024;14(11):4914-4933. https://doi.org/10.1016/j.apsb.2024.07.019.
10 Xu Q, Du YQ, Chen PP, et al. Computation assisted chemical study of photo-induced late-stage skeleton transformation of marine natural products towards new scaffolds with biological functions. *Chin Chem Lett*. 2025;36(5): 110141. https://doi.org/10.1016/j.cclet.2024.110141.
11 Gao CL, Song JQ, Yang ZN, et al. Chemoproteomics of marine natural product naamidine J unveils CSE1L as a therapeutic target in acute lung injury. *J Am Chem Soc*. 2024;146(41):28384-28397. https://doi.org/10.1021/jacs.4c09695.
12 Cui YY, Jin Y, Sun RN, et al. The first discovery of marine polyoxygenated cembranolides as potential agents for the treatment of ulcerative colitis. *J Med Chem*. 2024;67(14):12248-12260. https://doi.org/10.1021/acs.jmedchem.4c00950.
13 Zhang XY, Su MZ, Zhu MX, et al. The biologically and ecologically important natural products from the Chinese sea hare *Bursatella leachii*: structures, stereochemistry and beyond. *Chin J Nat Med*. 2024;22(11):1030-1039. https://doi.org/10.1016/s1875-5364(24)60611-4.
14 Xu Q, Yan BY, Wang HF, et al. Total synthesis of nocarterphenyl A, 2-dehydroxymethylnocarterphenyl A and nocarterphenyl D produced by marine *Nocardiopsis* spp. *J Nat Prod*. 2025;88(11):2710-2718. https://doi.org/10.1021/acs.jnatprod.5c01038.
15 Tao XY, Wang HR, Wang Q, et al. Marine natural product chagosendine C induces cuproptosis in colorectal cancer cells by targeting FDX1. *J Am Chem Soc*. 2025;147(41):37089-37103. https://doi.org/10.1021/jacs.5c07917.
16 Carbone M, Li Y, Irace C, et al. Structure and cytotoxicity of phidianidines A and B: first finding of 1,2,4-oxadiazole system in a marine natural product. *Org Lett*. 2011;13(10):2516-2519. https://doi.org/10.1021/ol200234r.
17 Jiang CS, Fu Y, Zhang L, et al. Synthesis and biological evaluation of novel marine-derived indole-based 1,2,4-oxadiazoles derivatives as multifunctional neuroprotective agents. *Bioorg Med Chem Lett*. 2015;25(2): 216-220. https://doi.org/10.1016/j.bmcl.2014.11.068.
18 Zhang L, Jiang CS, Gao LX, et al. Design, synthesis and *in vitro* activity of phidianidine B derivatives as novel PTP1B inhibitors with specific selectivity. *Bioorg Med Chem Lett*. 2016;26(3):778-781. https://doi.org/10.1016/j.bmcl.2015.12.097.
19 Labriere C, Elumalai V, Staffansson J, et al. Phidianidine A and synthetic analogues as naturally inspired marine antifoulants. *J Nat Prod*. 2020;83(11): 3413-3423. https://doi.org/10.1021/acs.jnatprod.0c00881.
20 Brogan JT, Stoops SL, Lindsley CW. Total synthesis and biological evaluation of phidianidines A and B uncovers unique pharmacological profiles at CNS targets. *ACS Chem Neurosci*. 2012;3(9):658-664. https://doi.org/10.1021/cn300064r.
21 Xie HX, Wang YH, Zhang JH, et al. Design, synthesis and biological evaluation of marine phidianidine-inspired derivatives against oxidized ldl-induced endothelial injury by activating Nrf2 anti-oxidation pathway. *Bioorg Chem*. 2022;120:105606. https://doi.org/10.1016/j.bioorg.2022.105606.
22 Xu Q, Zhao N, Liu J, et al. Design, synthesis and *in vitro* biological evaluation of marine phidianidine derivatives as potential anti-inflammatory agents. *Bioorg Med Chem*. 2022;71:116936. https://doi.org/10.1016/j.bmc.2022.116936.
23 Liu J, Li H, Chen KX, et al. Design and synthesis of marine phidianidine derivatives as potential immunosuppressive agents. *J Med Chem*. 2018;61 (24):11298-11308. https://doi.org/10.1021/acs.jmedchem.8b01430.
24 O'Daniel PI, Peng Z, Pi H, et al. Discovery of a new class of non-*β*-lactam inhibitors of penicillin-binding proteins with Gram-positive antibacterial activity. *J Am Chem Soc*. 2014;136(9):3664-3672. https://doi.org/10.1021/ja500053x.
25 Barbachyn MR. Identification of a 1,2,4-oxadiazole with potent and specific activity against *Clostridioides difficile*, the causative bacterium of *C. difficile* infection, an urgent public health threat. *J Med Chem*. 2023;66(20):13888-13890. https://doi.org/10.1021/acs.jmedchem.3c01778.
26 Clinical and Laboratory Standards Institute. *Methods for Dilution Antimicrobial Susceptibility Tests for Bacteria that Grow Aerobically, Approved Standard*, 9^{ed} edition (document M7–A7), 2018, Wayne, PA, USA.
27 Jia J, Zheng MX, Zhang CW, et al. Killing of Staphylococcus aureus persisters by a multitarget natural product chrysomycin A. *Sci Adv*. 2023;9(31):5995. https://doi.org/10.1126/sciadv.adg5995.
28 Chang TP, Chen ZF, Sheng LS, et al. Unanticipated quinoline modification on vancomycin as an effective atrategy to alter the antibacterial profile and combat multidrug resistance. *J Am Chem Soc*. 2025;147(46):42670-42684. https://doi.org/10.1021/jacs.5c14268.s001.